

Physics-based Electromigration Assessment for Power Grid Networks

Xin Huang[†], Tan Yu[†], Valeriy Sukharev[§] and Sheldon X.-D. Tan[†]

[†]Department of Electrical Engineering, University of California, Riverside, CA 92521, USA

[§]Mentor Graphics Corporation, Fremont, CA 94538, USA

xhuan009@ucr.edu, tyu008@ucr.edu, valeriy.sukharev@mentor.com, stan@ee.ucr.edu

ABSTRACT

This paper presents a novel approach and techniques for physics-based electromigration (EM) assessment in power delivery networks of VLSI systems. An increase in the voltage drop above the threshold level, caused by EM-induced increase in resistances of the individual interconnect segments, is considered as a failure criterion. It replaces a currently employed conservative weakest segment criterion, which does not account an essential redundancy for current propagation existing in the power-ground (p/g) networks. EM-induced increase in the resistance of the individual grid segments is described in the approximation of the recently developed physics-based formalism for void nucleation and growth. A statistical approach to calculation of the void nucleation times in the group of branches comprising the interconnect tree is implemented. As a result, p/g networks become time-varying linear networks. A developed technique for calculating the hydrostatic stress evolution inside a multi-branch interconnect tree allows to avoid optimistic prediction of the time to failure (TTF) made with the Blech-Black analysis of individual branches of interconnect tree. Experimental results obtained on a number of IBM benchmark circuits validate the proposed methodology.

Categories and Subject Descriptors

B.8.2 [Performance and Reliability]: Performance Analysis and Design Aids

General Terms

Algorithm, Reliability

Keywords

electromigration, hydrostatic stress, power grid, MTTF

1. INTRODUCTION

Electromigration-induced reliability threats become more significant with technology scaling. The problem becomes more severe for power delivery networks as they experience large unidirectional currents and thus are more susceptible

Permission to make digital or hard copies of all or part of this work for personal or classroom use is granted without fee provided that copies are not made or distributed for profit or commercial advantage and that copies bear this notice and the full citation on the first page. Copyrights for components of this work owned by others than ACM must be honored. Abstracting with credit is permitted. To copy otherwise, or republish, to post on servers or to redistribute to lists, requires prior specific permission and/or a fee. Request permissions from Permissions@acm.org.

DAC '14, June 01-05, 2014, San Francisco, CA, USA.

Copyright 2014 ACM 978-1-4503-2730-5/14/06 ...\$15.00

<http://dx.doi.org/10.1145/2593069.2593180>.

to EM effects than signal wires characterized by bidirectional currents. Continuous increase in the die size accompanied by reduction of the metal line cross sections and, hence by increase of the current densities governed by a technology scaling, results in an increasingly difficult EM signoff when the traditional EM checking approaches are employed. In these approaches, the EM-induced failure rates of the individual interconnect lines are considered as a measure of EM induced reliability and, in the extreme end, a mean time-to-failure (MTTF) of the weakest segment is accepted as a measure for the whole chip life-time. It results in a very conservative design rules for the current densities that can be used in the chip design for a particular technology node in order to avoid EM failure.

A very different way to EM assessment can be proposed from the positions of interconnect functionality, when the failure means its inability to function properly. There are two major functions of the chip interconnect: providing a connectivity between different parts of design for a signal propagating, and supplying a voltage. EM can degrade both these functions by degrading the conductivity of the individual segments of the interconnect circuits. The difference is in the types of electrical currents employed in these two cases. Indeed, the signal lines carrying bidirectional or pulsed currents are characterized by very long times to the EM-induced failure. It is caused by a repetitive increase and decrease of the mechanical stress at the line ends, caused by the excessive atom accumulation and depletion governed by the electron wind force and stress gradient. In contrast, power lines carrying unidirectional currents can fail in much shorter times due to continuous stress buildup under the EM effects. Thus, we can conclude that EM induced chip failure is happening mostly when the degrading p/g network leads to a severe IR drop problem. It means that loss of performance, which is a parametric failure, should be considered as the practical criterion of the EM-induced failure. It is clear that a structure of the power grid, which is characterized by high level of redundancy, can affect the kinetics of failure development. Indeed, due to redundancy, the failures of some of interconnect segments do not necessarily result in a critical IR drop on the p/g grid causing an electrical malfunction [4, 10]. Thus, more accurate and less pessimistic full-chip EM assessment requires new methods dealing with the grid structure and redundancy.

An accurate EM assessment assumes a calculability of transient current densities and temperatures in each p/g segment. A complexity of extraction of these distributions is exacerbated by an uncertainty in workload in modern chips. The complex multi-modal behavior results a dependency of the power dissipated by different blocks on the modes of operation. It means that current densities and temperatures in different interconnect segments should be estimated for different workloads and should be used for prediction

of MTTF happening in different scenarios including worst-case conditions for voltage drop [4]. Robust methodology of the full-chip EM assessment requires availability of accurate physics based models for void/hillock initiation and evolution responsible for a time-dependent resistance degradation of the p/g nets. Currently employed statistical Black's equation [2]:

$$MTTF = Aj^{-n} \exp\{E_a/kT\} \quad (1)$$

which calculates the segment MTTF based on known current densities (j) and temperatures (T), is the subject of growing criticism. Here, k is the Boltzmann's constant, E_a is the EM activation energy. The symbol A is a constant, which depends on a number of factors, including grain size, line structure and geometry, current density, thermal history, etc. Black has determined the value of n as equals to 2. However, it is a today's common understanding that n depends on residual stress and current density [6], and its value is highly controversial. In addition, as it was shown in a number of experiments, see for example [6], E_a is a function of the current density. All these observations make rather controversial the widely accepted methodology of calculating the MTTF at use condition, represented by chip operational current density and temperature, while using n and E_a determined at the stressed (accelerated) condition, characterized by high current densities and elevated temperatures as shown in Eq. (2).

$$MTTF_{use} = MTTF_{stress} \left(\frac{j_{stress}}{j_{use}} \right)^n \exp \left\{ \frac{E_a}{k} \left(\frac{1}{T_{use}} - \frac{1}{T_{stress}} \right) \right\} \quad (2)$$

Employments of the Blech limit [3]:

$$(j \times l) \leq (j \times l)_{crit} = \frac{\Omega \sigma_{crit}}{eZ\rho} \quad (3)$$

for the filtration of immortal segments, is also required a serious justification. Here, l is the segment length, Ω is the atomic volume, e is the electron charge, eZ is the effective charge of the migrating atoms, ρ is the wire electrical resistivity, σ_{crit} is the critical stress needed for the failure precursor nucleation (void/hillock). Condition of immortality Eq. (3) means the highest hydrostatic stresses developed at the line end(s) at the steady state, when atomic flux generated by stress gradient in the metal line compensates the atomic flux caused by the electrical current, are smaller than the corresponding critical stresses. It should be mentioned that the Blech limit is valid only for lines with the ends blocking the atomic diffusion. EM-induced accumulation of the hydrostatic stress exceeding the critical stresses responsible for void nucleation or the liner rupture, followed by metal extrusion into an inter metal dielectric (hillock formation), can happen only in interconnect segments with both or any one line end blocking atomic diffusion. A widely practiced decomposition of the multi-branch segments, also known as interconnect trees [7], on individual branches and applying the immortality condition to these individual branches makes the EM assessment over optimistic. While all individual branches can satisfy the condition of immortality, the interconnect tree can be mortal [7]. Hence, new physics-based MTTF compact model, which is free of all discussed flaws related to the Blech-Black formulation, should be developed.

This paper describes a novel methodology for power grid EM assessment, which addresses: (i) interconnect tree-based stress and EM analysis techniques, (ii) methodology of assessment of the overall reliability of the p/g grid, accounting its high level of redundancy.

2. ELECTROMIGRATION FUNDAMENTALS

EM is a physical phenomenon of the migration of metal atoms along a direction of applied electrical field. Atoms (either lattice atoms or defects/impurities) migrate toward the anode end of metal wire along the trajectory of conducting electrons. This oriented atomic flow, which is caused mostly by the momentum exchange between atoms and the conducting electrons, results in metal density depletion at the cathode, and a corresponding metal accumulation at the anode ends of the metal wire. The rate of EM-induced atom migration, as defined by the Nernst-Einstein equation, depends on the atomic diffusivity, meaning different materials are characterized by different rates of EM. Typical interconnect metals, such as copper (Cu) and aluminum (Al), are prone to EM, due to their high self-diffusivity. Refractive metals, such as tungsten, tantalum, and titanium, demonstrate strong resistance to EM. Everywhere, in the text below, the interconnect tree means a continuously connected, highly conductive metal within one layer of metallization, terminated by diffusion barriers. Thin layers of refractive metals form these diffusion barriers for Cu atoms, preventing them from diffusing into inter-layer (ILD) and inter-metal dielectrics (IMD). When metal wire is embedded into a rigid confinement, which is the case with interconnect metallization, the wire volume changes (induced by the atom depletion and accumulation due to migration) create tension at the cathode end and compression at the anode ends of the line. Over time, the lasting unidirectional electrical load increases these stresses, as well as the stress gradient along the metal line.

As it was mentioned above, the stress generated inside the embedded metal wire due to momentum exchange between lattice atoms and conduction electrons is a prime cause of void and hillock formation at the opposite ends of the wire. In addition to mentioned above nucleation of void at the cathode end of the wire, where a divergence in atomic flux happens (atom flux is terminated at the barrier interface), many voids are nucleated down to the polycrystalline metal line toward the anode end at any location characterized by the atom flux divergence. These are the triple points formed by intersections between grain boundaries (GB) and barrier layers, or contacts between three neighbor grains (Fig. 1(a) and Fig. 1(b)). It is known that atoms diffuse much faster along GB and interfaces than through the grain interiors, making GBs and interfaces the major venues for EM. Those triple points where the number of outward diffusion channels exceeds the number of inward channels can develop depletion in metal density, leading to possible void nucleation. Nucleated voids, depending on the local texture of neighboring grains, can grow in size or disappear. As shown in Fig. 1(c), two major mechanisms of void growth are: (i) scavenging the vacancies that migrate to the void due to the stress gradient between the void surfaces (zero stress) and the surrounding metal (tensile stress), (ii) agglomeration of voids traveling along the metal line toward the cathode end (against the electron flow) due to the capillarity effect. GBs with different crystallographic orientations are characterized by different atomic diffusivities. This variation, together with a random distribution of grain sizes inside metal lines, makes it clear why the identical metal lines, characterized by same geometries and same electrical load, demonstrate different times-to-failure (TTF). This TTF represents the instant in time when an increase in line electrical resistance caused by the void growth reaches a critical level (say, a 10% increase over the original value).

Degradation of the electrical resistance of interconnect segment can be derived from the solution of kinetics equation describing the time evolution of stress in the intercon-

nect segment [8, 5, 12, 13]. Indeed, the obtained instance in time when stress reaches the critical value $\sigma = \sigma_{crit}$, indicates the void nucleation time; extracted kinetics of the void volume evolution governs the evolution of the segment electrical resistance. While being successful in simulating the

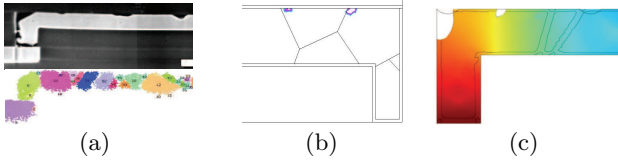


Figure 1: (a): TEM picture of voids nucleated at the top interface, [13], (b) and (c): simulated kinetics of the void nucleation at the triple points and growth (electron flow from right to left), (c): simulated growth of the line corner void by scavenging the vacancy flux and agglomerating with the small voids drifting along the top interface [13].

EM related physics in the frame of the finite-element analysis (FEA) [13], this type of modeling cannot be employed for the purpose of the analysis of stress evolution caused by the current load in hundreds of millions interconnect segments. A reason is the enormous size of the computational problem. To address this problem, the physics-based analytical compact model considering the void nucleation time and kinetics of void size evolution should be developed.

3. THE NEW PHYSICS-BASED EM ANALYSIS METHOD

3.1 Nucleation phase and nucleation time

Development of such analytical formulation was proposed by Korhonen [8] and further developed by other researchers; see for example [5, 12]. Since the atomic flux divergence results in the volumetric strain, it is easy to derive the one dimensional diffusion-like equation for the hydrostatic stress field $\sigma(x, t)$ [8]:

$$\frac{\partial \sigma}{\partial t} = \frac{\partial}{\partial x} \left[\kappa \left(\frac{\partial \sigma}{\partial x} + \frac{eZ\rho j}{\Omega} \right) \right] \quad (4)$$

Here, $\kappa = D_a B \Omega / kT$, where D_a is the atomic diffusivity, and B is the bulk modulus. Solution of this initial-boundary value problem is the infinite series [8]. Approximate value of void nucleation time (t_{nuc}) extracted from this solution, which is determined as an instant in time when stress at the cathode end of the line ($x = -l/2$) reaches σ_{crit} , corresponds well to an analytical formulation of t_{nuc} derived from the approximate solution of continuity equations for evolution of vacancy and plated atom concentrations (see, for example [13]) in the confined 1D line [14]:

$$t_{nuc} \approx \tau^* e^{\frac{E_V}{kT}} e^{-\frac{f\Omega}{kT} (\sigma_{Res} + \frac{eZ\rho l}{4\Omega} j)} \ln \left\{ \frac{\frac{eZ\rho l}{4\Omega} j}{\sigma_{Res} + \frac{eZ\rho l}{4\Omega} j - \sigma_{crit}} \right\} \quad (5)$$

where $\tau^* = \frac{l^2}{D_0} e^{\frac{E_D}{kT}} \frac{kT}{\Omega B}$. Here, E_V and E_D are the activation energy of vacancy formation and diffusion, f is the ratio of volumes occupied by vacancy and lattice atom. It was assumed that the metal segment was characterized by the residual stress of $\sigma_{Res} = \sigma_T + (B/9)(R/\delta) \exp\{-E_V/kT_{ZS}\}$ when electrical stressing was applied. Here, σ_T is the thermal stress developed in the metal line confined in the IMD/IMD dielectric during cooling from the zero stress temperature T_{ZS} down to the temperature of use condition, $(B/9)(R/\delta)$.

$\exp\{-E_V/kT_{ZS}\}$ is an additional stress generated by vacancy relaxation to the equilibrium concentration corresponding to new stress value and temperature [14], R is the mean grain size, and δ is the GB thickness. Dependence of t_{nuc} on grain size allows one to introduce a simple statistical model for void nucleation at the line cathode edge. Employment of the lognormal distribution as the experimentally proven distribution of the grain size in the polycrystalline metal line provides different t_{nuc} for the geometrically identical metal lines loaded with the same electrical current densities.

3.2 Growth phase and wires resistance change rate

The second phase is the void size growth: voids are formed at t_{nuc} and grow at $t > t_{nuc}$. The wire resistance starts to increase over the time in the growth phase. As a result, the p/g network becomes a time-varying network and its voltage drops will keep changing over the time.

Since the drift velocity of the void edge relates to atomic flux as $\vartheta = \Omega j$ [15], we can express it as:

$$\vartheta = \frac{D}{kT} eZ\rho j \quad (6)$$

Kinetics of the wire resistance change can be approximately described as:

$$\Delta r(t) = \vartheta(t - t_{nuc}) \left[\frac{\rho_{Ta}}{h_{Ta}(2H + W)} - \frac{\rho_{Cu}}{HW} \right] \quad (7)$$

Here ρ_{Ta} and ρ_{Cu} are the resistivity of the barrier material (Ta/TaN) and copper, W is the line width, H is the copper thickness, and h_{Ta} is the barrier layer thickness.

An accurate description of the void growth is pretty complicated. The growth dynamics involves an atom exchange between void surface and triple points formed by copper/liner interfaces and void surface, as well a transfer of atoms along the void surface to feed the previous flux. The surface diffusion can be a limiting step of the void volume extension that can be responsible for the absence of the large statistical scatter observed in experiments [15].

3.3 Tree-based EM analysis method

The physics-based EM model discussed above was developed for a single interconnect line confined by IMD/ILD dielectric. But, as it was mentioned already, the modern p/g networks consist of large segments/interconnect trees as shown in Fig. 2. These segments can have multiple voltage input/output and current source ports represented by interlayer vias and contacts. The major difference between iso-lines and individual branches of interconnect trees is an absence of blocking boundaries at one or both ends of the branches. It prevents atoms from accumulation/depletion and eliminates related stress buildup at the unblocked branch ends, and hence makes traditional immortality assessment groundless. Fig. 3 shows distributions of the current density and hydrostatic stress developed in the three terminals interconnect tree. Two vias are used as the electron flow inlets and one positively biased as outlet. The hydrostatic stress obtained from the solution of the system of partial-differential equations with the FEA tool COMSOL [1] demonstrates the two-slope distribution resulted by the intra branch atom diffusion. It makes clear that in order to explain such distribution, the stress analysis should be performed in the tree as a whole instead of a single wire [7]. We will demonstrate below how it affects the developed EM assessment flow.

Let's assume that for a given interconnect tree, a distribution of the DC current densities and the current flow directions are known, and the void-less steady state was achieved.

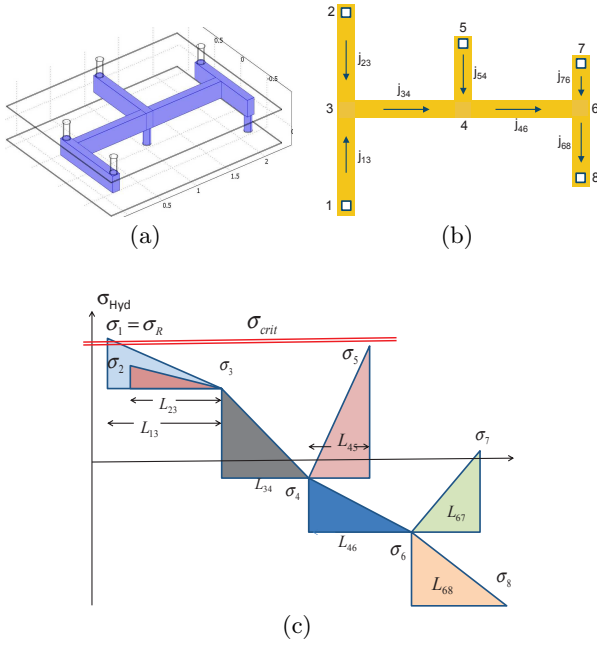


Figure 2: (a) Interconnect segment confined by diffusion barriers/liners; (b) Example of an interconnect tree. (c) Hydrostatic stress distribution in the interconnect tree.

It provides a simple estimation of the stress distribution along each branch:

$$\sigma_i^c - \sigma_j^a = \Delta\sigma_{ij} = -\frac{eZ\rho(j_{ij}L_{ij})}{\Omega} \quad (8)$$

Here, σ_i^c and σ_j^a are the hydrostatic stresses at the cathode and anode ends of the ij -branch. Eq. (8), together with the atom conservation condition Eq. (9), allow obtaining the stresses at all nodes of the tree as shown in Fig. 2(c).

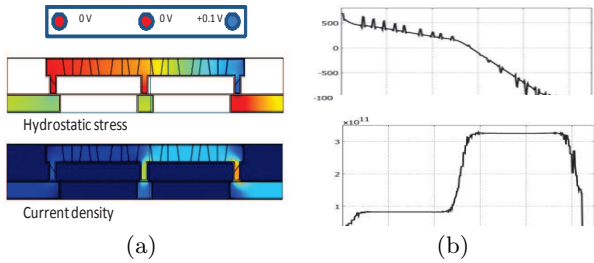


Figure 3: Hydrostatic stress (a) and current density (b) distributions along the top metal line.

$$\sum_{i=1}^k \left(\sigma_i - \left[\sigma_T + \frac{B}{3} \left(\frac{R_i}{\delta} \right) e^{-\frac{E_V}{kT}} + \frac{eZ\rho(j_{ij}L_{ij})}{2\Omega} \right] \right) L_{ij} = 0 \quad (9)$$

If any stress exceeds σ_{crit} , then the time for void nucleation at the cathode, characterized by the biggest stress σ_m , is:

$$t_{nuc}^m \approx \frac{L_{max/min}^2}{2D_0} e^{\frac{E_V + E_D}{kT}} \frac{kT}{\Omega B} \exp\left\{ -\frac{f\Omega\sigma_m(j_1, j_2, \dots, j_n)}{kT} \right\} \times \ln\left\{ \frac{\sigma_m(j_1, j_2, \dots, j_n) - \sigma_T - \frac{B}{3} \left(\frac{R_i}{\delta} \right) e^{-\frac{E_V}{kT}}}{\sigma_m(j_1, j_2, \dots, j_n) - \sigma_{crit}} \right\} \quad (10)$$

Eq. (10) is the extension of the Eq. (5) for the case of multi-branch segment. Here, $\sigma_m(j_1, j_2, \dots, j_n)$ is the steady state stress at the cathode end of the (m, k) branch characterized by the biggest tensile stress in the considered interconnect tree, and n is the number of sub-segments, $L_{max/min}$ is the distance inside the segment, which connects the cathode (maximal tensile stress) with anode (maximal compressive or minimal tensile stress). In a case when several cathodes reveal stresses exceeding σ_{crit} , the nucleation time still should be calculated for the cathode with the biggest stress.

4. NEW POWER GRID RELIABILITY ANALYSIS METHOD

In this section, we present the proposed new power grid reliability analysis method using the nucleation and growth concepts and physics-based EM models we discussed in the previous sections.

4.1 Power grid models

Because of the concern with the long-term average effects of the current, a DC model of the power grid is generally assumed [4]. As a result only the EM-induced kinetics of the power grid network resistances should be considered. Regarding the transient current sources, we will show how to compute the effective EM current and effective EM current sources later. In our problem formulation, each mortal wire, which is the subject to the EM impact, will start to change its resistance value upon achieving the nucleation time. As a result, we end up with the power grid systems, which is a linear, time-varying and driven by the DC effective currents. For a power grid networks with n nodes,

$$G(t) \times v(t) = I(t) \quad (11)$$

where $G(t)$ a $n \times n$ time-varying conductance matrix; $I(t)$ is transient current source vector; $v(t)$ is the corresponding vector of nodal voltages. In our problem, the time scale is the EM time scale, which can be months or years.

EM is a long-term cumulative failure phenomenon. The changes in the line current on very short time-scale in the normal operations of a chip are not very significant. As a result, the effective EM currents, which are constant DC currents, are computed. The effective-EM currents will give the same lifetime as the transient waveforms. It can be understood from the following. Eq. (4) provides the kinetics of the hydrostatic stress in the interconnect line caused by applied current. A simple integration provides:

$$\sigma(t, x) - \sigma_0 = \frac{\partial}{\partial x} \left[\int_0^t \kappa \frac{\partial \sigma}{\partial x} dt + \kappa \frac{eZ\rho}{\Omega} \int_0^t j dt \right] \quad (12)$$

It means that under assumptions made for derivation of the Eq. (4) in [8], the stress distribution at any particular instant in time is governed by the time integral of the applied current density. This can be used as a justification of replacing the current waveforms with the time averaged DC current. For most general cases of both uni-directional and bi-directional currents, we have the following effective-EM current density [9]:

$$J_{trans,EM,eff} = \frac{1}{T} \left(\int_0^T J^+(t) dt - \psi \int_0^T |J^-(t)| dt \right) \quad (13)$$

where $J^+(t)$ is the current density from one side. ψ is the EM recovery factor, which is determined by experiments. So if we only have unidirectional current, which is the case of p/g network, the effective-EM current density essentially

is the time-averaged current density. Furthermore, we compute the effective EM current sources in a similar way, which will generate the same effective current densities in each wire segments so that only one DC analysis is required for EM analysis at each EM time point.

4.2 New analysis method flow

Algorithm 1 New power grid EM-induced reliability analysis algorithm

!h

Input: power grid networks with current inputs, time step, technology parameters

Output: The time reaching the threshold voltage drop (MTTF).

- 1: Compute the initial effective EM current density.
- 2: Compute the steady state distributions of hydrostatic stress inside each interconnect tree.
- 3: Find all suspicious branches with the tensile stress larger than the critical one. Compute the nucleation time $t_0 = \min\{t_{nuc}^i\}$ for the most vulnerable branch (with the largest stress).
- 4: Start the analysis from time $t = t_0$. Branch with nucleation time t_0 enters the growth phase.
- 5: **while** the largest voltage drop \leq threshold **do**
- 6: Move to next instant in time $t := t + \Delta t$, update the wire resistances for all wires in the growth phase.
- 7: Perform the DC analysis of the power grids. Recompute the current densities of each branch.
- 8: Identify new branches with the stresses exceeding the critical one.
- 9: Calculate the nucleation time t_{nuc}^i for all suspicious branches in the nucleation phase. If $\min\{t_{nuc}^i\} \leq t$, the corresponding branch steps into the growth phase.
- 10: **end while**
- 11: Output t and the failed segment.

Now we present the new EM-induced reliability analysis algorithm and flow for p/g networks. In our formulation of the dynamic p/g networks, the wire resistance begins to change (increase) starting with the nucleation time (t_{nuc}). After this, their resistance changes will be computed by Eq. (7). First we compute initial current densities $j_{0,mn}$ for each branch of every tree. Then, by using the proposed tree-based EM analysis method, we obtain the stresses for all branches in all trees. Then, we identify the trees, which are the subjects for void nucleation: hydrostatic stress at any of the tree nodes is larger than the σ_{crit} . Then, we compute the set of t_{nuc}^i for all suspicious branches. Branch characterized by the largest stress and smallest t_{nuc} among others sets up the initial (starting) time t_0 , which is indicated by $t_0 = \min\{t_{nuc}^i\}$ in the step 3 in the algorithm, and the branch will be included in the growth phase pool. It should be mentioned that the randomization procedure must be exercised for calculating t_{nuc}^i for the identical branches. After this, we move to next step $t_1 = t_0 + \Delta t$. The chosen time-step Δt should be small enough to detect approximately an instant in time when the critical stress is developed in any branch of any segment. We update power grid conductance matrix G due to resistance change in the wire in the growth phase, re-compute current densities j for each wire of each tree again, and repeat the previous steps: stress calculation, identification of the branches satisfying $\sigma > \sigma_{crit}$, putting the most vulnerable branch into growth phase pool if reaches its t_{nuc} , and moving to the next step: $t_2 = t_1 + \Delta t$. We continue this process until the voltage drops at one or more nodes reach the given threshold such as 10% of the supply

voltage. We identify this instant in time as the mean time to failure (MTTF) of the whole p/g network.

It should be mentioned that this flow doesn't account for generation of the void saturated volume [7], which develops when growing void consumes all volumetric deformation generated by thermal stress and by redistribution of atoms removed from the space occupied by growing void. Analysis of this phenomenon will require longer simulation run and will result longer MTTF in comparison with one calculated with neglecting the effect of void volume saturation. Since the MTTFs obtained in the last case for different p/g nets were noticeable longer than those calculated in accordance with the traditional approach, the former case was reserved for the future analysis.

5. NUMERICAL RESULTS AND DISCUSSIONS

The proposed EM assessment method is implemented in C++ on a 2.4GHz Linux server with 36 GB memory and validated by the IBM power grid benchmark circuits [11], which has both power networks and ground networks. The power networks are used to test our method and their source current values are modified to ensure that the initial voltage drop of any node is smaller than the threshold value. In this work, we assume the interconnect material is copper and the power grid circuit fails when the largest voltage drop exceeds $10\%V_{DD}$. Parameters used in our model are listed in Table I. Table II shows the power grid MTTF obtained from both Black's equation and our proposed approach. In Black's equation based analysis, Eq. (2) is used to estimate the MTTF of single metal line, where $T_{stress} = 600K$, $j_{stress} = 3MA/cm^2$, $Ea = 0.83eV$ and $MTTF_{stress}$ is obtained from Eq. (5) under stressed condition (use condition characteristics are the same as characteristics used in our predictive work). Two different Black's equation based models are used to compare with the proposed method. One

Table 1: Parameters used in our model

Parameter	Value	Parameter	Value
E_V	0.82eV	T	373K
E_D	0.65eV	Z	10
f	0.6	σ_T	400MPa
B	1×10^{11}	σ_{crit}	600MPa
R/δ	3×10^3	T_{ZS}	653K

Table 2: Comparison of Power Grid MTTF using black's equation and our model

Power Grid		Time to Failure (yrs)			CPU time of Our Method
		Black's Equation		Proposed model	
Name	Nodes	Series	Mesh		
IBMPG2	61797	7.82	10.67	15.66	54.66min.
IBMPG3	407279	15.77	19.95	27.61	19.61hr.
IBMPG4	474836	12.58	23.68	29.20	19.93hr.
IBMPG5	497658	6.34	11.1	23.05	54.87min.
IBMPG6	807825	9.53	13.97	17.80	32.52hr.
IBMPGNEW1	715022	13.64	17.50	22.48	6.89hr.
IBMPGNEW2	715022	12.44	18.77	20.12	5.99hr.

is series model, under which the circuit is considered to have failed as soon as any branch fails. The other is mesh model that takes redundancy into account, defining the circuit fails when it cannot deliver required amount of voltage. From the experimental results, we can observe that the Black's equation based series model would lead to a too pessimistic prediction. The MTTF estimated by Black's equation based mesh model is more conservative than our model due to the fact that it assumes infinite resistance after the predicted MTTF of each branch while actually the metal line continues to conduct voltage after MTTF with increasing resistance. The voltage drop distribution at the instant in time

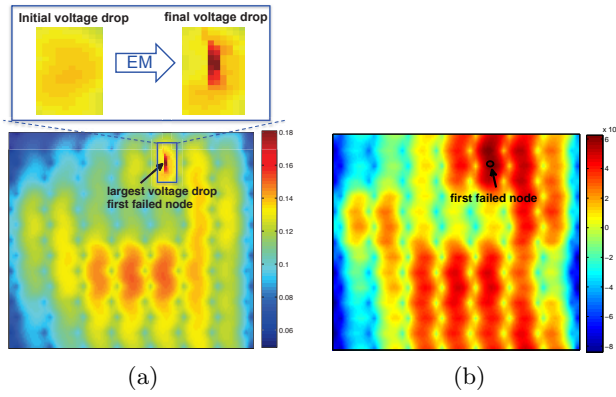


Figure 4: (a) Voltage drop (V) distribution and (b) the predicted steady state hydrostatic stress (Pa) distribution by the initial current density in IBMPG2.

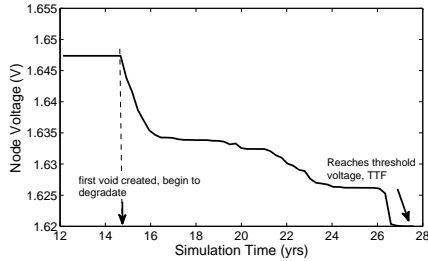


Figure 5: Voltage of the first failed node in different simulation time

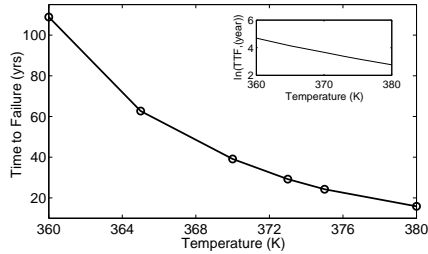


Figure 6: Effect of temperature on MTTF

when failure of the power grid network has happened and the steady state hydrostatic stress distribution predicted by initial current density in the metal layer that directly connects to the underlying logic blocks are shown in Fig. 4(a) and Fig. 4(b) respectively. From the experimental result, we observe that the first failure is most likely to happen at the nodes where the initial hydrostatic stress is large. The growth time depends on the circuit's particular topology. However, from our experiments, which may not have a general character, we found that the void nucleation time is typically larger or comparable to the growth time. So the segments with larger stress are more likely to nucleate void and, since the void grows is almost independent on stress, the voltage drop at these places will likely exceed with time the threshold value.

Node voltage keeps changing with time after creation of the first void in the network and its value can be tracked as shown in Fig. 5. Effect of different average chip temperatures on p/g network's MTTF is investigated. From Fig. 6, the experimental result reveals that MTTF obtained from our proposed method obeys the same functional dependencies as the Black's equation, which is the Arrhenius dependence on temperature. So reducing the temperature can efficiently suppress the EM effect.

6. CONCLUSION

In this work, a new physics-based EM modeling and assessment method has been proposed and implemented for the power grid networks of VLSI systems. The proposed method accounts for the redundancy of the power grids, while assuming that the circuit is deemed to have failed if it cannot function properly. Void nucleation and growth are considered for assessing the resistance growth. The new EM modeling method accounts the statistical nature of the EM phenomenon due to a random grain size distribution. It can also account the thermal and other process-induced residual stresses, which is ignored by the Black's equation based EM assessment. Developed technique allows to assess the evolution of hydrostatic stress inside a multi-branch interconnect tree for more accurate prediction of the TTF in comparison with the traditional Blech-Black analysis of individual branches of the interconnect tree. The experimental results show that the Black's equation based analysis in either weak segment or mesh approximations would lead to more pessimistic results compared with the proposed method. It also reveals that for the IBM p/g circuits the EM induced failure is more likely to happen at the place where the initial steady state stress is large.

7. REFERENCES

- [1] "Comsol multiphysics," <http://www.comsol.com>.
- [2] J. R. Black, "Electromigration-A Brief Survey and Some Recent Results," *IEEE Transactions on Electron Devices*, vol. 16, no. 4, pp. 338-347, 1969.
- [3] I. A. Blech, "Electromigration in thin aluminum films on titanium nitride," *Journal of Applied Physics*, vol. 47, no. 4, pp. 1203-1208, 1976.
- [4] S. Chatterjee, M. B. Fawaz, and F. N. Najm, "Redundancy-Aware Electromigration Checking for Mesh Power Grids," in *Proc. Int. Conf. on Computer Aided Design (ICCAD)*, 2013.
- [5] J. J. Clement, "Reliability analysis for encapsulated interconnect lines under dc and pulsed dc current using a continuum electromigration transport model," *Journal of Applied Physics*, vol. 82, no. 12, pp. 5991-6000, 1997.
- [6] M. Hauschildt, C. Hennesthal, G. Talut, O. Aubel, M. Gall, K. B. Yeap, and E. Zschech, "Electromigration early failure void nucleation and growth phenomena in Cu and Cu(Mn) interconnects," in *2013 IEEE International Reliability Physics Symposium (IRPS)*. IEEE, 2013, pp. 2C.1.1-2C.1.6.
- [7] S. P. Hua-Riege and C. V. Thompson, "Experimental characterization and modeling of the reliability of interconnect trees," *Journal of Applied Physics*, vol. 89, no. 1, pp. 601-609, 2001.
- [8] M. A. Korhonen, P. Borgesen, K. N. Tu, and C. Y. Li, "Stress evolution due to electromigration in confined metal lines," *Journal of Applied Physics*, vol. 73, no. 8, pp. 3790-3799, 1993.
- [9] K.-D. Lee, "Electromigration recovery and short lead effect under bipolar and unipolar-pulse current," in *IEEE International Reliability Physics Symposium (IRPS)*, 2012, pp. 6B.3.1-6B.3.4.
- [10] V. Mishra and S. S. Sapatnekar, "The impact of electromigration in copper interconnects on power grid integrity," in *Design Automation Conference (DAC), 2013 50th ACM / EDAC / IEEE*, 2013, pp. 1-6.
- [11] S. R. Nassif, "Power grid analysis benchmarks," in *Proc. Asia South Pacific Design Automation Conf. (ASPDAC)*, 2008, pp. 376-381.
- [12] M. E. Sarychev, Y. V. Zhitnikov, L. Borucki, C.-L. Liu, and T. M. Makhviladze, "General model for mechanical stress evolution during electromigration," *Journal of Applied Physics*, vol. 86, no. 6, pp. 3068-3075, 1999.
- [13] V. Sukharev, A. Kteyan, E. Zschech, and W. D. Nix, "Microstructure Effect on EM-Induced Degradations in Dual Inlaid Copper Interconnects," *IEEE Transactions on Device and Materials Reliability*, vol. 9, no. 1, pp. 87-97, Mar. 2009.
- [14] V. Sukharev, "Beyond Black's Equation Full-Chip EM/SM Assessment In 3D IC Stack," pp. 1-29, Apr. 2013.
- [15] Z. Suo, *Reliability of Interconnect Structures*, ser. Comprehensive Structural Integrity. Amsterdam: Elsevier, 2003, vol. 8.